Superconductivity and Field-Induced Magnetism in $Pr_{2-x}Ce_xCuO_4$ Single Crystals

J. E. Sonier,[1,5] K. F. Poon,[1] G. M. Luke,[2,5] P. Kyriakou,[2] R. I. Miller,[3,*] R. Liang,[3,5] C. R. Wiebe,[2] P. Fournier,[4,5] and R. L. Greene[6]

[1]*Department of Physics, Simon Fraser University, Burnaby, British Columbia V5A 1S6, Canada*
[2]*Department of Physics & Astronomy, McMaster University, Hamilton, Ontario L8S 4M1, Canada*
[3]*Department of Physics and Astronomy, University of British Columbia, Vancouver, British Columbia V6T 1Z1, Canada*
[4]*Département de Physique, Université de Sherbrooke, Québec J1K 2R1, Canada*
[5]*Canadian Institute for Advanced Research, Toronto, Ontario, Canada*
[6]*Center for Superconductivity Research, Department of Physics, University of Maryland, College Park, Maryland 20742, USA*

(Received 11 February 2003; published 29 September 2003)

We report muon-spin rotation and relaxation (μSR) measurements on single crystals of the electron-doped high-T_c superconductor $Pr_{2-x}Ce_xCuO_4$. In a zero external magnetic field, superconductivity is found to coexist with dilute Cu spins that are static on the μSR time scale. In an applied field, we observe a μ^+-Knight shift that is primarily due to the magnetic moment induced on the Pr ions. Below the superconducting transition temperature T_c, an additional source of local magnetic field appears throughout the volume of the sample. This finding is shown to be consistent with field-induced antiferromagnetic ordering of the Cu spins. Measurements of the temperature dependence of the in-plane magnetic penetration depth λ_{ab} in the vortex state are also presented.

DOI: 10.1103/PhysRevLett.91.147002 PACS numbers: 74.25.Ha, 74.72.–h, 76.75.+i

While there now exists a large body of convincing experimental work on high-T_c superconductors with hole-type carriers, the intrinsic properties of the electron-doped cuprates $R_{2-x}Ce_xCuO_4$ ($R \equiv$ La, Pr, Nd, Sm, or Eu) have remained very elusive. Part of the problem stems from the difficulty of preparing single phase superconducting samples. An additional complication is the presence of both Cu and rare-earth (R) moments. The interplay between these two magnetic sublattices has been studied extensively in the undoped parent compounds R_2CuO_4 [1]. In Ce-doped samples, magnetic exchange interactions involving the CuO_2 planes may play a role in the superconducting state, where the pairing symmetry is still a matter of considerable debate. Although recent phase sensitive [2] and angle-resolved photoemission [3] experiments are consistent with d-wave pairing symmetry, measurements of thermodynamic quantities such as the in-plane magnetic penetration depth λ_{ab} generally do not show the expected linear temperature dependence at low T that is characteristic of a ''clean'' superconductor. Many of the early results for $\lambda_{ab}(T)$ in electron-doped cuprates were obtained in the Meissner phase of $Nd_{2-x}Ce_xCuO_4$ (NCCO) thin films and single crystals. While these results favored s-wave symmetry [4–6], it has since been recognized that the paramagnetism of the Nd ions strongly affects the low-T behavior of $\lambda_{ab}(T)$ [7–10]. Consequently, attention has shifted primarily to the $Pr_{2-x}Ce_xCuO_4$ (PCCO) system, where crystal electric field (CEF) splitting of the Pr^{3+} $J = 4$ manifold results in a nonmagnetic singlet ground state. However, recent measurements of $\lambda_{ab}(T)$ in PCCO thin films and crystals using a variety of techniques have not yielded consistent results [8–14].

To avoid extrinsic effects related to the sample surface, we have utilized muon-spin rotation and relaxation (μSR), which is a local magnetic probe and one of the few techniques capable of measuring $\lambda_{ab}(T)$ in the vortex state. Attempts to accurately measure $\lambda_{ab}(T)$ in NCCO by μSR have been precluded by the considerable Nd-moment contribution to the muon-spin depolarization rate [15]. In this Letter, we report on the first μSR study of superconducting PCCO single crystals.

We studied three single crystals of PCCO grown by a directional solidification technique in Al_2O_3 crucibles using a CuO-based flux [16]. Reduction of oxygen to induce superconductivity was achieved by encapsulating each single crystal in polycrystalline PCCO in the presence of flowing Ar at 900–1000 °C (Ref. [17]). Here we report on representative data from one of the single crystals, noting that qualitatively similar results were obtained in a partial μSR study of the other two. The crystal was 0.07 mm thick, having an $\hat{a}$-$\hat{b}$ plane area of $\sim$6.5 mm^2 and a mass of 3.74 mg. Although resistivity measurements indicate a T_c value of 25(1) K, bulk susceptibility $\chi^{\perp}$ measurements show that the diamagnetic signal assumes a constant value below $\sim$16 K (see Fig. 1).

The measurements were carried out on the M15 and M20B positive muon (μ^+) beam lines at TRIUMF, Canada. In a μSR experiment, the spin of the implanted μ^+ precesses at a frequency $\omega_\mu = \gamma_\mu B_\mu$, where B_μ is the local field at the μ^+ site and $\gamma_\mu = 13.5534$ kHz G^{-1} is the muon gyromagnetic ratio. The PCCO single crystals are the smallest samples studied to date by conventional μSR. A special arrangement of scintillator detectors inside a He gas-flow cryostat was used to eliminate the signal from muons that did not stop in the sample.

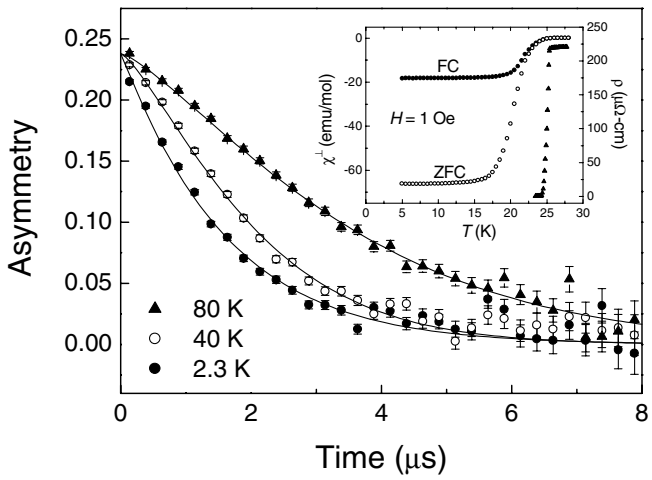

FIG. 1. Time evolution of the asymmetry [i.e., $A(t) = AP(t)$, where A is the signal amplitude] in zero external field at $T =$ 80, 40, and 2.3 K. The initial muon-spin polarization was parallel to the CuO_2 layers. Inset: Temperature dependence of the resistivity (solid diamonds), and the bulk susceptibility at $H = 1$ Oe under FC and ZFC conditions.

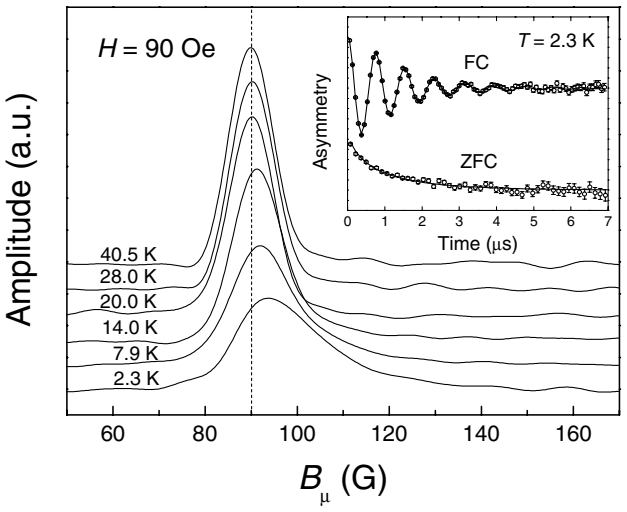

FIG. 2. FFTs of the muon-spin precession signal in PCCO taken under FC conditions. The dashed vertical line indicates the external field $H = 90$ Oe. Inset: Asymmetry spectra taken at $T = 2.3$ K under both FC and ZFC conditions.

Measurements were taken both in zero external field (ZF) and in a transverse field (TF) geometry, with the applied field H directed perpendicular to the CuO_2 planes.

In ZF, the muon-spin polarization $P(t)$ is relaxed by magnetic moments of electronic and nuclear origin. As shown in Fig. 1, the relaxation rate of the ZF-μSR signal increases with decreasing T. The absence of discrete frequency oscillations indicates that there is no onset of spontaneous magnetic order at temperatures above 2.3 K. Measurements carried out in a longitudinal-field geometry [18] at $T = 25$ K indicate that the muon-spin relaxation is due to randomly oriented local magnetic fields, that are static on the μSR time scale. The time spectra in Fig. 1 are well described by a power-law relaxation function $G(t) = e^{-(\Lambda t)^{\beta}}$, where β decreases from 1.4 at $T =$ 50 K to 1.0 at $T = 2.3$ K. Such behavior is consistent with *dilute* Cu moments (or Cu-spin clusters) in a background of concentrated nuclear dipoles [19].

TF-μSR and magnetization measurements were carried out under both field-cooled (FC) and zero-field cooled (ZFC) conditions. Typical asymmetry spectra are shown in the inset of Fig. 2. In the ZFC case, pinning at the sample edges prevents flux from entering the bulk at $T = 2.3$ K and $H < 300$ Oe. Thus, the ZFC time spectrum in Fig. 2 resembles that observed in ZF. For ZFC measurements above 300 Oe, flux fully penetrates the sample at $T = 2.3$ K, but pinning centers prevent the formation of an equilibrium vortex lattice configuration. In contrast, the FC method generally yields a regular pattern of vortices. Fast Fourier transforms (FFT) of the muon-spin precession signal taken under FC conditions at $H = 90$ Oe are shown in Fig. 2. The FFT provides an approximate picture of the internal magnetic field distribution $n(B)$ [20]. Above T_c, the linewidth is due to the field distribution created by the electronic and nuclear magnetic moments. The linewidth is observed to increase with increasing H, indicating an inhomogeneous spread in local magnetic susceptibility due to sample demagnetization effects, and perhaps spatial variations in O and Ce concentration. For this reason, we focused our study on the low H regime. As shown in Fig. 2, the line shape broadens further and becomes asymmetric below T_c. These are characteristics of the inhomogeneous field distribution created by a lattice of vortices.

The stopping site of the μ^+ has previously been identified in the related undoped parent compound Nd_2CuO_4 as near an O(2) oxygen atom midway between adjacent CuO_2 layers [21]. Consistent with this site assignment, the TF-μSR signal in PCCO shows a single well-resolved signal with an average frequency shifted relative to the Larmor precession frequency of μ^+ in vacuum. The corresponding μ^+-Knight shift is

$$K_{\mu}^{\perp} = \frac{B_0 - \mu_0 H}{\mu_0 H} - 4\pi\left(\frac{1}{3} - N\right)\rho_{\mathrm{mol}}\chi^{\perp}, \qquad (1)$$

where B_0 is the average internal magnetic field sensed by the muons, the second term is a correction for Lorentz and bulk demagnetization fields, $\rho_{\mathrm{mol}} = 0.017\,44$ mol/cm^3 is the molar density of PCCO, and $N \approx 1$ is the demagnetization factor for a thin platelike crystal. Figure 3 shows that $K_{\mu}^{\perp}$ (i.e., the local magnetic susceptibility) scales linearly with $\chi^{\perp}$ above T_c, indicating that the relative frequency shift is not induced by the μ^+. Susceptibility measurements have established that the field-induced moment on the Pr ion dominates the magnetic response of PCCO in the normal state [22]. As shown in the inset of Fig. 3, χ is highly anisotropic due to strong CEF effects.

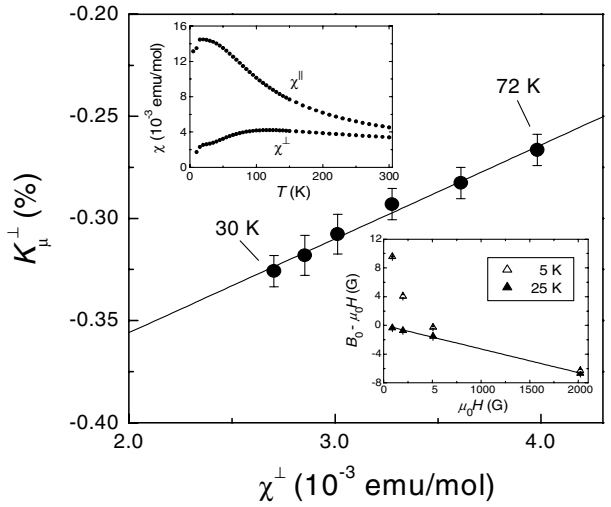

FIG. 3. $K_\mu^\perp$ vs $\chi^\perp$ at $H = 3$ kOe. The solid line is a fit to Eq. (2). Left inset: Temperature dependence of the bulk susceptibility at $H = 10$ kOe applied parallel ($\chi^\parallel$) and perpendicular ($\chi^\perp$) to the CuO_2 layers. Right inset: Magnetic field dependence of $B_0 - \mu_0 H$ at $T = 5$ K and 25 K. Each data point at $T = 5$ K represents a single FC measurement.

The Pauli paramagnetic susceptibility χ_0 of the conduction electrons gives rise to a T-independent Knight shift, $K_0 = A_0\chi_0$, where A_0 is the contact hyperfine coupling constant. The field-induced moment on the Pr ions results in a T-dependent Knight shift $K_f^\perp$ consisting of two contributions: (i) the dipole-dipole interaction between the localized Pr $4f$ moments and the μ^+, and (ii) an indirect Rudermann-Kittel-Kasuya-Yosida (RKKY) interaction, producing a spin polarization of the conduction electrons at the μ^+ site. Assuming the Cu-moment contributions to be negligible, $K_\mu^\perp$ at the axial symmetric μ^+ site is given by

$$K_\mu^\perp \approx K_0 + K_f^\perp = K_0 + (A_c + A_{dip}^{zz})\chi_f^\perp, \qquad (2)$$

where A_c and A_{dip}^{zz} are the contact hyperfine and dipolar coupling constants, respectively, and $\chi_f^\perp \approx \chi^\perp - \chi_0$. At the μ^+ site, we calculate $A_{dip}^{zz} = -0.66$ kG/μ_B. The solid line in Fig. 3 is a fit to Eq. (2), yielding $A_c = 3.23$ kG/μ_B and $K_0 > -4480$ ppm.

Below T_c, there is a substantial increase of B_0 that nearly coincides with the increase of the diamagnetic signal under FC conditions (see Fig. 4). This cannot be explained by the reduction of χ_0 that arises from the formation of Cooper pairs. We first considered the possibility that the increased field is a manifestation of the so-called *paramagnetic Meissner effect* [23], but the diamagnetic response observed in both the FC and ZFC magnetization does not support this interpretation. A second possible origin, speculated to be responsible for magnetorestriction enhancements [24] and diamagnetic shifts of B_0 [25] in the superconducting state of the $RBa_2Cu_3O_{7-\delta}$ system, is screening currents induced in the CuO_2 layers by large $R \equiv$ Gd, Er moments. This is highly unlikely here, as the induced Pr moment at $H = 90$ Oe is weak—as evidenced by the normal state measurements, where $B_0 - \mu_0 H < -0.3$ G.

A third possibility is that the vortices nucleate magnetic order. The solid curve in Fig. 4 is a fit assuming $B_0^S = [(B_0^N)^2 + (B^*)^2]^{1/2}$, where B_0^S (B_0^N) denotes B_0 in the superconducting (normal) state, and $B^* \approx 43$ G and 28 G, at 5 and 10 K, respectively. This indicates that the additional field B^* that appears at the μ^+ site is directed parallel to the basal plane. Dipolar-field calculations show that this is consistent with the noncollinear Cu-spin structure determined by neutron scattering in the parent compound Pr_2CuO_4, where the ordered Cu moment is $0.4\mu_B$ [26]. In particular, precise quantitative agreement is obtained at $T = 5$ K with the Cu spins canted $\sim 12°$ out of the CuO_2 plane, as previously determined by μSR in insulating PCCO [27]. Since nearly all the muons see an increase in B_μ (see Fig. 2), AF order of the Cu spins appears to be stabilized throughout the bulk of our PCCO single crystals by a *low density* of vortices [28].

The in-plane magnetic penetration depth λ_{ab} can be determined from the TF-μSR time spectra as described in Ref. [20]. In the normal state, the muon-spin precession signal is well described by the polarization function $P(t) = e^{-(\sigma t)^\alpha}\cos(\omega_\mu t + \phi)$, where $\alpha \approx 1.6$ and σ is the temperature-dependent depolarization rate. The TF-μSR time spectra below T_c were well fit to

$$P(t) = e^{-(\sigma t)^\alpha}\int n_v(B)\cos(\gamma_\mu B t + \phi)\, dB, \qquad (3)$$

where $n_v(B)$ is the field distribution of a hexagonal vortex lattice derived from Ginzburg-Landau theory, and σ is due primarily to the effects of the magnetic moments—which occur on a length scale that is 10^3 times smaller than λ_{ab}. Using Eq. (3) with a fixed value for the

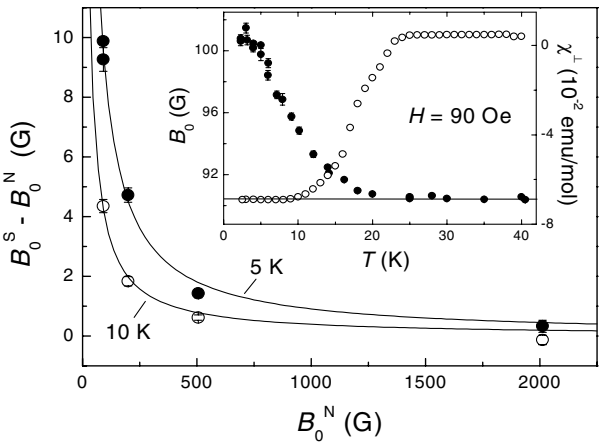

FIG. 4. $B_0^S(T) - B_0^N$ vs B_0^N at $T = 5$ K (solids circles) and 10 K (open circles). The solid curves are described in the text. Inset: Temperature dependence of B_0 and $\chi^\perp$ taken under FC conditions.

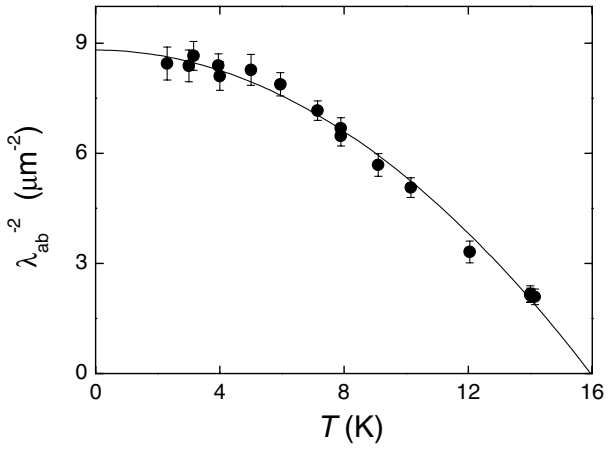

FIG. 5. λ_{ab}^{-2} vs T in PCCO at $H = 90$ Oe. The solid curve is a fit described in the text.

coherence length ξ_{ab}, we find that σ scales as $1/(T - \theta)$, where $\theta = -18(5)$ K. At low H, only a small fraction of the implanted muons stop near the vortex cores. Consequently, the analysis is not very sensitive to the value of ξ_{ab}. For example, increasing ξ_{ab} from 30 to 60 Å changes the fitted value of $\lambda_{ab}(0)$ by less than 2%.

Figure 5 shows the temperature dependence of λ_{ab}^{-2}. The absence of data below $T = 2.3$ K forbids an accurate determination of the limiting temperature dependence of $\lambda_{ab}^{-2}(T)$. The solid curve is a fit to $\lambda_{ab}^{-2}(T) = \lambda_{ab}^{-2}(0)[1 - (T/T_c)^2]$, yielding $T_c = 15.9(2)$ K and $\lambda_{ab}(0) = 3369(73)$ Å. The values of T_c and $\lambda_{ab}(0)$ indicate that the bulk of our sample is primarily underdoped. For example, Meissner state measurements in Ref. [13] on an underdoped PCCO film reported $\lambda_{ab} = 3100$ Å. This same study showed evidence for a crossover from s-wave to d-wave behavior in the underdoped regime.

In conclusion, we have observed the onset of static magnetic order in the superconducting state of PCCO single crystals with a weak field applied perpendicular to the CuO_2 layers. The appearance of AF order in the vortex state of high-T_c superconductors is a key prediction of several theories [29,30], and there are now a number of experiments performed at higher H providing evidence for the effect. That AF order is observed in PCCO at such low fields may be partly due to the close proximity of the superconducting and AF phases in electron-doped cuprates. However, sample inhomogeneity may play a role here and in underdoped $La_{2-x}Sr_xCuO_4$, where the field-induced AF order is clearly not confined to the vortex cores [31]. Last, our measurements of $\lambda_{ab}^{-2}(T)$ in the vortex state are consistent with Meissner state results on underdoped PCCO. However, a unique determination of the low-temperature behavior by μSR awaits the availability of larger single crystals.

We are especially grateful to R. F. Kiefl and D. E. MacLaughlin for insightful discussions. This work was supported by the Natural Sciences and Engineering Research Council of Canada, and in the United States by National Science Foundation Grant No. DMR 01-02350.

*Present address: Department of Physics & Astronomy, University of Pennsylvania, Philadelphia, PA 19104, USA.

[1] R. Sachidanandam *et al.*, Phys. Rev. B **56**, 260 (1997).
[2] C. C. Tsuei and J. R. Kirtley, Phys. Rev. Lett. **85**, 182 (2000).
[3] N. P. Armitage *et al.*, Phys. Rev. Lett. **86**, 1126 (2001).
[4] D.-H. Wu *et al.*, Phys. Rev. Lett. **70**, 85 (1993).
[5] A. Andreone *et al.*, Phys. Rev. B **49**, 6392 (1994).
[6] S. M. Anlage *et al.*, Phys. Rev. B **50**, 523 (1994).
[7] J. R. Cooper, Phys. Rev. B **54**, R3753 (1996).
[8] L. Alff *et al.*, Phys. Rev. Lett. **83**, 2644 (1999).
[9] J. D. Kokales *et al.*, Phys. Rev. Lett. **85**, 3696 (2000).
[10] R. Prozorov, R.W. Giannetta, P. Fournier, and R. L. Greene, Phys. Rev. Lett. **85**, 3700 (2000).
[11] H. C. Ku *et al.*, Physica (Amsterdam) **364C–365C**, 285 (2001).
[12] J. A. Skinta, T. R. Lemberger, T. Greibe, and M. Naito, Phys. Rev. Lett. **88**, 207003 (2002).
[13] J. A. Skinta, M.-S. Kim, T. R. Lemberger, T. Greibe, and M. Naito, Phys. Rev. Lett. **88**, 207005 (2002).
[14] A. Biswas *et al.*, Phys. Rev. Lett. **88**, 207004 (2002).
[15] G. M. Luke *et al.*, Physica (Amsterdam) **282C–287C**, 1465 (1997).
[16] J. L. Peng, Z.Y. Li, and R. L. Greene, Physica (Amsterdam) **177C**, 79 (1991).
[17] M. Brinkmann, T. Rex, H. Bach, and K. Westerholt, J. Cryst. Growth **163**, 369 (1996).
[18] A. Kanigel *et al.*, Phys. Rev. Lett. **88**, 137003 (2002).
[19] M. R. Crook and R. Cywinski, J. Phys. Condens. Matter **9**, 1149 (1997).
[20] J. E. Sonier, J. H. Brewer, and R. F. Kiefl, Rev. Mod. Phys. **72**, 769 (2000).
[21] G. M. Luke *et al.*, Phys. Rev. B **42**, 7981 (1990).
[22] M. F. Hundley *et al.*, Physica (Amsterdam) **158C**, 102 (1989).
[23] M. Sigrist and T. M. Rice, Rev. Mod. Phys. **67**, 503 (1995).
[24] J. Zieglowski *et al.*, Z. Phys. B **71**, 429 (1988).
[25] R. L. Lichti, D.W. Cooke, and C. Boekema, Phys. Rev. B **43**, 1154 (1991).
[26] I.W. Sumarlin *et al.*, Phys. Rev. B **51**, 5824 (1995).
[27] J. Akimitsu *et al.*, Hyperfine Interact. **85**, 187 (1994).
[28] At $T = 2.3$ K, $H = 90$ Oe, magnetic order should reduce the initial asymmetry A by ~19%. However, because of the simultaneous occurrence of magnetic order and a vortex lattice, and systematic uncertainties introduced by the specialized apparatus, A is poorly determined.
[29] D. P. Arovas, A. J. Berlinsky, C. Kallin, and S. C. Zhang, Phys. Rev. Lett. **79**, 2871 (1997).
[30] E. Demler, S. Sachdev, and Y. Zhang, Phys. Rev. Lett. **87**, 067202 (2001).
[31] B. Lake *et al.*, Nature (London) **415**, 299 (2002).